Available online at www.sciencedirect.com

SciVerse ScienceDirect

Journal of the European Ceramic Society 32 (2012) 2113–2120

www.elsevier.com/locate/jeurceramsoc

Chemical treatment on alumina–zirconia composites inducing apatite formation with maintained mechanical properties

M.G. Faga [a,*], A. Vallée [b], A. Bellosi [a], M. Mazzocchi [a], N.N. Thinh [b], G. Martra [b], S. Coluccia [b]

[a] National Council of Research, Institute of Science and Technology for Ceramics, Strada delle Cacce 73, 10135 Torino, Via Granarolo 64, 40018 Faenza (RA), Italy
[b] Department of Inorganic Physic and Materials Chemistry, Via Giuria 7, 10125 Torino, Italy

Received 11 May 2011; received in revised form 30 November 2011; accepted 13 December 2011
Available online 28 February 2012

Abstract

Alumina–zirconia composites with submicrometric grain size were surface modified with the purpose to induce bioactivity using several chemical treatments. Among them, a quick attack by phosphoric acid induced on Zirconia Toughned Alumina (80–20 wt%) the formation of apatite-like calcium phosphate phases after immersion in simulated body fluid, indicating bioactivity induction. Such a treatment does not reduce the strength, hardness and ageing properties of this ceramic material, making it a suitable method for biomedical applications. Surface properties, topography and microstructure of oxide ceramics are also discussed.

Keywords: Composites; Al_2O_3; ZrO_2; Apatite; Mechanical properties

1. Introduction

The excellent mechanical and tribological properties together with biocompatibility of alumina and yttria stabilized zirconia materials (Y-TZP) ceramics[1] have led to consider them as a good choice for preparing orthopaedics and dental clinical implants. Despite the fact that the future of (Y-TZP) materials has been questioned in the recent years, due to the report of failures of their application in vivo[2–4] a large number of studies still regards them as promising biomaterial.[5,6] The problem was caused by the low temperature degradation (LTD) of zirconia, the so-called ageing process. Basically, the process involves transformation of metastable tetragonal crystallites into the monoclinic phase.[7–12] Chevalier et al.[9] suggested an incubation-nucleation-growth mechanism for the transformation. Once the transformation occurs, the process continuously proceeds from the surface to the bulk of yttria stabilized zirconia materials, resulting in a volumetric expansion followed by failure.[9] It is well known that zirconia materials transform most rapidly at temperature ranging between 200 and 300 °C. However, at low temperatures, the process can be enhanced by the presence of water, which is available in vivo.[9,13] Fundamentally, penetration of water radicals into zirconia lattice leads to the formation of tensile stresses in zirconia surfaces. Consequently, the activation barrier for the transformation is lowered, and the phase transition is promoted.[14]

A modern trend to improve the LTD resistance is to seek for materials processing leading to alumina–zirconia composites. Two kinds of composites can be prepared: alumina matrix reinforced with zirconia particles (ZTA), and zirconia matrix reinforced with alumina particles (ATZ). The "driving ideal" is to isolate zirconia grains in the lattice structure from others by alumina grains to avoid the propagation process. The combination of alumina and zirconia allows to compensate the moderate toughness of alumina and the ageing effect of zirconia.

The mechanical and tribological properties of different ZTA and ATZ compositions have been reported in many studies during the last years.[15–20] Higher toughness can be obtained for particular composites than for pure alumina or zirconia. It has been also shown that when the percentage of ZrO_2 is kept under the 22 wt%,[21,22] ageing phenomena do not occur independently from the grain size, and recently it was described that no surface

* Corresponding author. Tel.: +39 0113977616; fax: +39 011346288.
E-mail address: m.faga@to.istec.cnr.it (M.G. Faga).

0955-2219/$ – see front matter © 2012 Elsevier Ltd. All rights reserved.
doi:10.1016/j.jeurceramsoc.2011.12.020

morphological changes occurred on a ZTA composite, indicating the absence of macroscopic effects.[23]

Despite the fact that ZTA seems to be a promising material on a point of view of ageing effect, ATZ has particularly good mechanical properties.

The mechanical stability is not the only requirement of a good implant material since it is also primordial for it to present a bioactivity for those applications requiring osteointegration. Bioactivity, in case of bone bonding materials, can be described as the ability to grow bonelike apatite on the materials surfaces.[24] It has been shown that apatite formation is induced by the presence of particular hydroxyl sites on the surface. The introduction of (OH) functional groups on the materials surfaces by acid and base treatments seems to represent a promising solution[25,26] to induce bioactivity. Such processes have allowed to grow apatite on the materials surfaces when they were immersed in the simulated body fluid (SBF).[24]

It is also known that the Al–OH functional group has no affinity for calcium and phosphate and do not induce apatite formation.[27] By contrast, zirconia gels with tetragonal or monoclinic structure were proved to effectively induce apatite nucleation[26,28] by the specific arrangement of the Zr–OH functional group which are a nucleation supply for apatite crystal formation. The work of Kokubo et al.[26] has shown that a zirconia composite (70 vol.% zirconia, 30 vol.% alumina) was able to form apatite layer on the surface after acidic or basic treatments. It is worth to be noted that the composite treated with H_3PO_4 5 M exhibited the highest apatite-forming rate.

Considering these facts, increasing zirconia content of the materials may improve their bioactivity. In spite of the fact that several studies reporting the possibility to induce bioactivity on the surface of zirconia-based materials are present, the influence of the treatments on the mechanical properties and ageing are not so widely investigated.

In this paper, ZTA and ATZ ceramics with submicrometric grain size were considered as suitable materials for dental and orthopaedic applications. The microstructure and mechanical properties have been studied before and after the treatment for the surface bioactivation.

2. Experimental

2.1. Ceramic preparation and characterization

High purity powders were used to produce the materials: Taimei Al_2O_3–16 wt%ZrO_2 (Taimicron) and Tosoh ZrO_2–20 wt%Al_2O_3 (TZ-3Y20AB), in form of "ready to press" powders, so that no additional mixing was done before pressing.

Green samples were obtained by linear pressuring at 80 MPa followed by Cold Isostatic Pressing under 200 MPa. The best conditions for sintering process were: heating 50 °C/h up to 700 °C, dweel for 2 h at 700 °C; heating of 100 °C/h up to temperature sintering of 1500 °C and dwell for 2 h at this temperature. The thermal expansion coefficients were measured up to 1300 °C; the densities of the sintered bodies were measured by Archimedes' method.

Furthermore, the following mechanical properties were considered: 4-pts flexural strength on 45_5_5 mm test bars (at least five specimens for each batch) for as fired materials and 25_2.5_2 for aged and treated ones; hardness by indentation method with a Vickers tip, 9.8 N of load, for 10 s, on at least five specimens for each batch for as fired materials; for treated and aged ceramics micro-hardness was measured with a nanoindentation tester (FISCHERSCOPE HM-2000) varying the load up to 0.5 N to evaluate the surface hardness. Also in this case a Vickers indenter, consisting of a four-sided diamond pyramid with a square base, was used for the measurement. Toughness was measured by indentation method with a Vickers tip, 98 N of load, for 10 s, with at least five measurements on each material and Young's modulus by resonant frequency method on at least three specimens for each batch, sized 43_5_2 mm using an H&P gain phase analyzer.

The slice model equation of Munz et al. was used to calculate toughness.

Flexural strength and hardness were measured on as fired, aged and treated samples.

The materials were studied without any polishing treatments, apart from samples for microstructure and XPS. The choice to avoid polishing was based to the fact that a higher surface contact is helpful for osteointegration. As for microstructure and XPS, polishing is required to have effective results. Polishing was done using diamond up to 1 μm of grain size.

Microstructure was analysed using a Scanning Electron Microscope; Zeiss EVO 50 equipped with Energy Dispersion Spectroscopy analyzer for elemental composition detection.

XPS analyses were collected on a SPECS (Phoibos MCD 150) X-ray photoelectron spectrometer. The source was Mg Kα radiation (1253.6 eV). The X-ray source having a 150 W (12 mA, 12.5 kV) electron beam power. The spot size of the irradiated region is 7×20 mm. The emissions of photoelectrons from the sample were analyzed at a take-off angle of 90° under UHV conditions. No charge compensation was applied during acquisition. After collection, the binding energies were calibrated on the Al 2p signal of Al_2O_3 having a binding energy BE = 74 eV. The accuracy of the reported binding energies (BEs) can be estimated to be ±0.1 eV. The XPS peak areas were determined after subtraction of a background. The atomic ratio calculations were performed after normalization using Scofield factors of element X. All spectrum processing was carried out using the Casa XPS v2.3.13 software (Casa Software Ltd.) package and Origin 7.1 (Origin Laboratory Corp.). The spectral decomposition was performed using Gaussian–Lorentzian (70%/30%) functions, and the FWHM is fixed for each given peak.

2.2. Samples treatment

The samples were ultrasonically washed in acetone, ethanol and deionized water and then immersed in H_3PO_4 or NaOH solution with different concentrations at 80–100 °C for times ranging between 4 and 24 h in autoclave or under atmospheric pressure. After the complete treatment, the samples were taken

out from solution, then washed in deionized water and finally dried at room temperature.

2.3. Bioactivation

Bioactivity evaluation of the untreated and treated samples was performed by immersing the materials in a modified simulated body fluid (1.5× SBF). The 1.5× SBF was prepared with ion concentration 1.5 times that of SBF as proposed by Kokubo and Takadama,[24] and its pH value was adjusted to 7.4 by the addition of HCl and Tris–hydroxymethyl-aminomethane. Each sample was immersed in 40 ml 1.5× SBF, kept at a constant temperature of 36.5 °C for 2 and 4 weeks. Observation by SEM-EDS of a layer with typical Ca/P ratio of apatite-like forms was used as a criterion for the samples bioactivity.

2.4. Ageing experiments

Ageing experiments were carried out in autoclave at a temperature of 134 °C and 2 bars at increasing time, up to 20 h (1 h in autoclave is theoretically equivalent to 3–4 years in vivo[9]).

Samples were located on a grid in the autoclave so that they were not soaked in water during the ageing, but only subjected to steam atmosphere. The influence of hydrothermal treatment on the tetragonal- monoclinic transformation was quantitatively evaluated by X ray diffraction. The specimens were scanned with Cu-Kα (45 kV–40 mA) radiation and Bragg angle varying from 26° to 34° by PANalytical X Pert PRO X-ray diffraction instrument. The monoclinic phase fraction X_m of zirconia was calculated using the Garvie and Nicholson method.

$$X_m = \frac{I_{m(\bar{1}\,1\,1)} + I_{m(1\,1\,1)}}{I_{m(\bar{1}\,1\,1)} + I_{m(1\,1\,1)} + I_{t(1\,0\,1)}}$$

where X_m is the m-ZrO_2 fraction.

$I_t(1\,0\,1)$, $I_m(1\,1\,1)$ and $I_m(1\,1\,1)$ are the integrated intensity corresponding to the tetragonal (1 0 1), monoclinic (−1 1 1) and monoclinic (1 1 1) planes, respectively.

The monoclinic volume V_m ratio is then given in the formula

$$V_m = \frac{1.311X_m}{1 + 0.311X_m}$$

We decided to use such method because it is often employed in the papers related to zirconia-based composites for biomaterials and, consequently, it allows an easy comparison with literature data.[29,30]

The zirconia phase transformation was then observed by Atomic Force Microscope (AFM) and Scanning Electron Microscopy (SEM). The same zone of the ATZ sample was imaged before and after ageing process. The AFM (Park System XE100) was using in non-contact mode. The scan size was $5 \times 5\,\mu m^2$ with a scan rate of 0.4 Hz. The measurements have been performed on polished and thermally etched sample on air. The measurements of average roughness (R_a) have been evaluated by images in five random areas on the sample.

The SEM images were obtained using the same instrument described in Section 2.1.

To observe the same zone in AFM and SEM, the sample was marked with a line scratch obtained with a progressive load from 10 to 50 N. In addition, to easily locate the area analyzed by AFM, a photo of the tip during the first AFM analysis was recorded. After the ageing process, the AFM tip was placed in the same area and several images were recorded to find the same zone observed on the unaged material, with the aim to clearly observe the ageing effect on the surface.

3. Results and discussion

3.1. Microstructure

The morphologies of the ZTA and ATZ composites are shown in Fig. 1. Both samples are made of submicrometric grains, with the darker and brighter grains representing the alumina and zirconia phases respectively. In particular, in the case of Al_2O_3–16 wt%ZrO_2 (ZTA), Al_2O_3 grains of $0.9 \pm 0.3\,\mu m$ and ZrO_2 grains of $0.3 \pm 0.1\,\mu m$ are present, while in the case of ZrO_2–20 wt%Al_2O_3 (ATZ) alumina and zirconia sizes are similar ($0.5 \pm 0.2\,\mu m$). In both cases, alumina and zirconia grains are homogeneously distributed. In the case of ZTA the alumina grains are bigger, probably because of the low proportion of zirconia, which has a pinning effect on alumina grains.

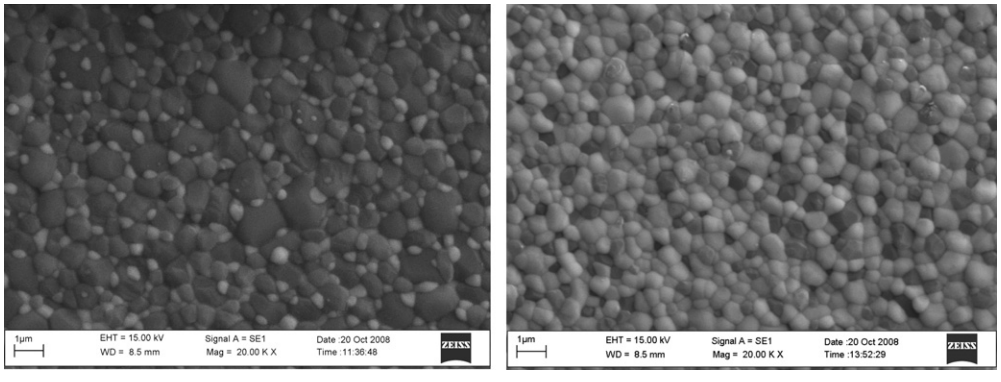

Fig. 1. Scanning Electron Microscopy images of (a) ZTA and (b) ATZ as fired.

Table 1
Physical and mechanical properties of ZTA, ATZ and monolithic materials.

Composition	Density (%)	Thermal expansion coefficient (m °C)	Hardness (GPa)	Toughness (MPa m$^{1/2}$)	Flexural strength (MPa)	Young modulus (GPa)
Al_2O_3–16 wt%ZrO_2	100	8.2	21.3 ± 1.5	3.9 ± 0.05	441 ± 24	363 ± 5
ZrO_2–20 wt% Al_2O_3	99.9	10.0	15.3 ± 0.9	7.1 ± 0.1	633 ± 127	245 ± 9
Al_2O_3[a]	99.9	7.8	24.0 ± 1.6	3.0 ± 0.1	229 ± 34	362 ± 4
ZrO_2[b]	100	11.0	14.5 ± 0.4	6.0 ± 0.3	615 ± 93	206 ± 4

[a] Al_2O_3 taimei.
[b] ZrO_2 tosoh, stabilized with 3 wt% of yttria.

3.2. Physical and mechanical properties

The composites properties are summarized in Table 1, where also features of monolithic materials are reported for comparison. The optimized materials processing led to fully dense materials. As a general remark, it can be observed that the composites exhibit a good compromise in terms of hardness and toughness if compared to monolithic materials.

In particular, the ATZ composite shows similar hardness and increased toughness if compared to pure zirconia. This indicates that the ATZ is more fracture-tolerant than the zirconia. This is a particular advantage because, in spite of the promising mechanical properties of pure zirconia, the risk of fracture remains an important problem.

As for the ZTA, which is expected to be stable in vivo because the zirconia percentage is only 16% in weight, its mechanical properties are interesting too. In fact, toughness and flexural strength are considerably better in comparison with monolithic alumina even if hardness is kept high. However, toughness and flexural strength are significantly lower than those found in the other composite, indicating a higher fragility of this material. It has to be noticed that a relevant standard deviation for ZTA is observed, mainly for the strength values, indicating that a reduction of defects have to be obtained by improving and controlling the materials processing.

3.3. Surface characterization

Before starting any chemical treatments, the oxide surface was characterized by XPS. The results obtained on ZTA and ATZ samples reveal the presence of aluminium, zircon, yttrium, oxygen and carbon atoms on the surfaces. The presence of carbon is originated from the surface contaminations related to the species spontaneously adsorbed from the air and the low level of nitrogen can come from the fabrication process of the two oxides. Other contaminants in very small amount (Na and Si) are also present, and they are probably related to traces of them in the starting powders or have been collected during the preparation procedure.

The spectra were calibrated on the Al 2p signal of Al_2O_3 having a binding energy BE = 74 eV.

The zircon peak presents one doublet with the component Zr $3d_{5/2}$ at 181.8 ± 0.1 eV. The binding energy difference of 2.4 eV between Zr $3d_{5/2}$ and Zr $3d_{3/2}$ peaks is in agreement with the binding energy of Zr^{4+} in pure zirconia.[31,32] The component Y $3d_{5/2}$ of the Yttrium doublet found at 157 ± 0.1 eV, with a difference of 2 eV with peak Y $3d_{3/2}$ is characteristic of the yttria tetragonal-ZrO_2 phase-stabilizer in YSZ.[33]

The O 1s peak results from four contributions at 529.7, 530.8, 532.0 and 533.3 ± 0.1 eV corresponding respectively to O^{2-} of the zirconia matrix (O1), to O^{2-} of the alumina matrix (O2), to the hydroxyl groups due to the water chemisorption solutions (O3), and to the hydrated surface layer of the material (O4).[34,35]

To estimate the amount of oxygen related to the contaminations of these samples, the C 1s peaks have been decomposed into five contributions at 284.7, 285.0, 286.3, 287.6 and 288.9 (±0.1 eV) related to C–C C–H, C–C(=O)OX, $C(-O)_2$, C–O and C–C(=O)OX, respectively[34,36] (cf. Fig. 2).

The oxygens associated with carbonaceous contaminations (involved in C–O or C=O bonds) are estimated to be 13 and 10% for the ZTA and ATZ, respectively. One can thus deduce the percentage of oxygen associated with the oxide and hydroxide layers and check the composition of the ZTA and ATZ surfaces.

The quantitative proportion of aluminium, zircon, yttrium and oxygen expected for ZTA and ATZ samples is calculated considering the amounts of ZrO_2, Al_2O_3 and Y_2O_3 used in the precursor mixture (Table 2).

The values calculated considering the stoichiometric ratio are very close to the experimental ones. These results provide evidence that chemical composition of the surface of ZTA and ATZ are very close to that of the bulk. One can moreover notes that the experimental Y percentage is higher than the expected one.

It is also remarkable to see the good agreement between the Intensity ratios of the O 1s contributions of the oxygen coming from the Zirconia matrix and coming from the Alumina matrix (0.14 for the ZTA and 1.79 for the ATZ) with the expected stoichiometric atomic ratio Zr/Al (0.08 for the ZTA and 1.66 for the ATZ) (cf. Fig. 3).

3.4. Chemical treatments

Various treatments with H_3PO_4 and NaOH at different concentrations, temperatures, during different times were

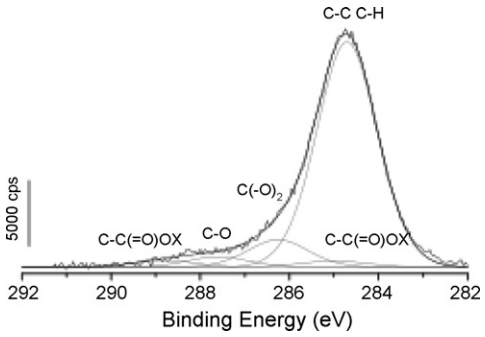

Fig. 2. C 1s peak deconvolution related to surface contaminants.

Table 2
Element percentage on the surface of ZTA and ATZ samples as calculated by XPS.

Elements	Atomic % in ZTA (calculated)	Atomic % in ZTA (XPS)	Atomic % in ATZ (calculated)	Atomic % in ATZ (XPS)	Atomic % in ATZ treated 4 h with H_3PO_4 (XPS)
Al	36.6	37.9	13.4	13.5	13.7
Zr	2.8	3.7	21.8	19.9	21.0
O	60.5	57.5	64.1	63.4	61.8
Y	0.1	0.9	0.7	3.2	3.5

considered to induce bioactivity on the surface of the both composites. The ability of these treatments to induce apatite formation on the surfaces has been tested by immersion in SBF. As reference, untreated and treated ZTA and ATZ materials were immersed in SBF solution for two and four weeks.

No apatite formation was observed for ZTA in any case, indicating that there is a threshold percentage of zirconia under that bioactivity is not induced.

Among the various treatments, only one (H_3PO_4 42 wt%, 80 °C, 4 h in autoclave) led to apatite-like formation in the case of ATZ after four weeks of immersion in SBF both in static and dynamic methods. The surface was almost completely covered by a layer of calcium phosphates, for which the ratio between Ca and P was 1.6, as expected for apatite forms.[37] Acicular morphology was found in each test (both static and dynamic). As indicated in Fig. 4c, apatite starts to grow preferably on zirconia grains, confirming that such oxide is more effective for apatite nucleation.[26] Furthermore, this aspect can justify why the composite containing a lower percentage of zirconia does not exhibit the same ability in promoting apatite formation. To check the effect of phosphoric acid on ATZ, XPS spectra were acquired on the samples after the treatment. The spectra were calibrated in the same way used for as fired samples. No remarkable differences were found with respect to the ATZ as fired in terms of Zr/Al ratio. Furthermore, no phosphorus peak has

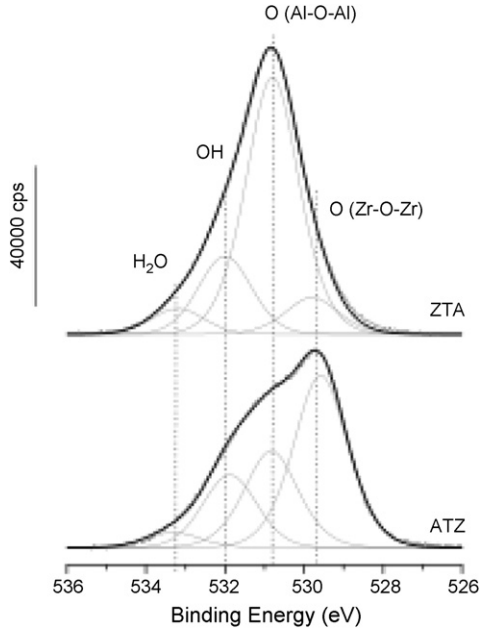

Fig. 3. O 1s peaks deconvolution for ZTA and ATZ as fired materials.

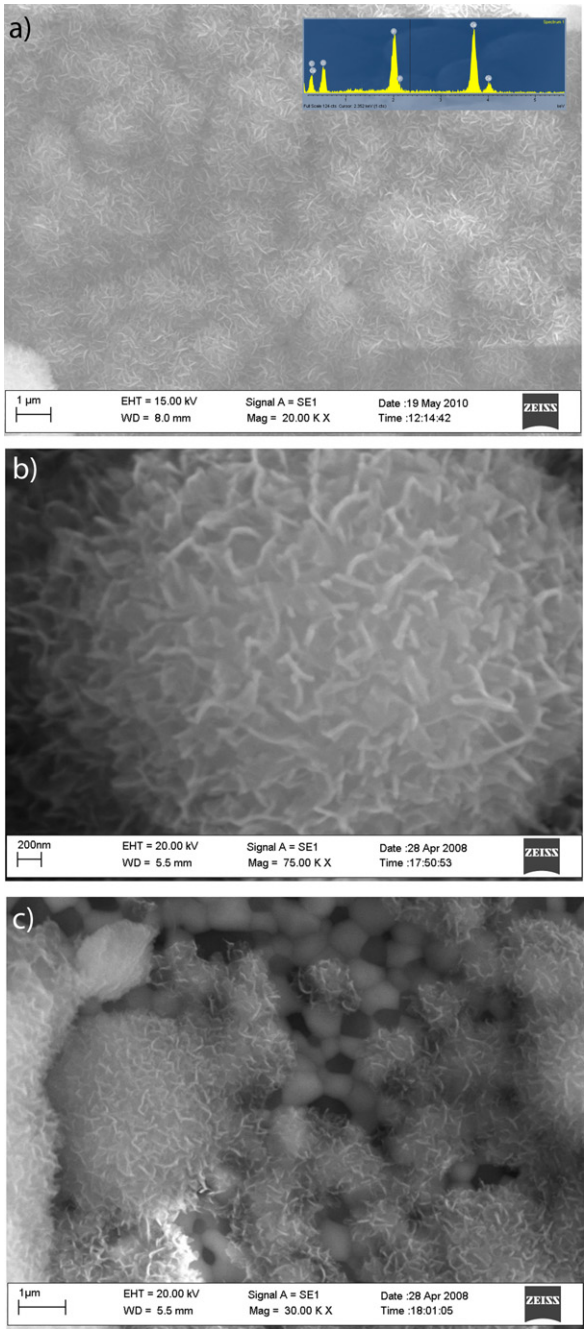

Fig. 4. SEM-EDS analysis of the ATZ sample after immersion for 4 weeks in SBF (a) morphology and EDS analysis of the apatite-like layer; (b) particular of the a; (c) interaction between phosphate phases and ATZ surface, indicating the preferential grew on Zirconia grains.

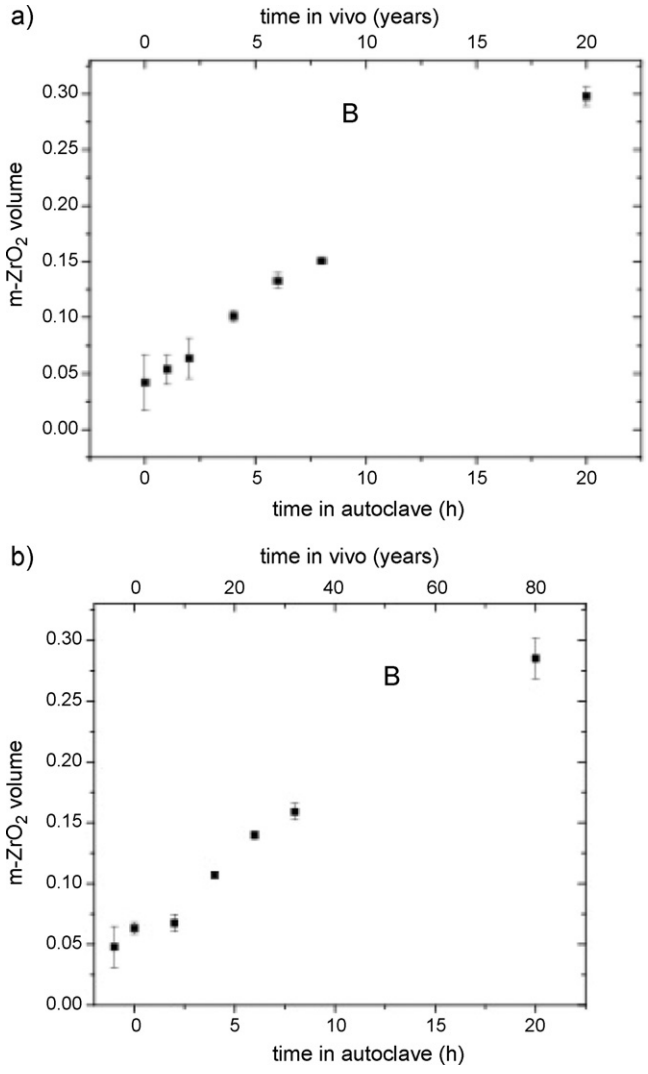

Fig. 5. Correlation between ageing time and m-ZrO_2 content in (a) as fired ATZ; (b) ATZ treated by H_3PO_4 for 4 h.

Table 3
Comparison of the Oxygen contributions for ZTA, ATZ and ATZ treated by phosphoric acid.

O1s components	ZTA	ATZ	ATZ 4 h H_3PO_4
$\%O_2$–(ZrO_2)	9.3	48.7	43.7
$\%O_2$–(Al_2O_3)	65.2	27.2	23.4
%OH	19.2	20.0	24.6
$\%H_2O$	6.3	4.1	8.3

been observed, indicating that no phosphate phase was formed. The deconvolution of O 1s peak revealed interesting differences between ATZ as fired and treated by phosphoric acid (Table 3). In last case, in fact, an increase of OH and water percentage was found. So probably the bioactivity observed in this sample has to be related to an increase of OH species on the surface, coming from a base–acid reaction between zirconia and phosphoric acid. The fact that the same treatment did not lead to a similar effect on alumina-rich sample confirms that alumina grains are not effective for apatite nucleation.

It is also important to note that the same treatment in beaker did not produce any effect on the bioactivity after the same time, suggesting that the pressure plays an important role in accelerating the kinetics of the surface modification.

3.5. ATZ ageing effect

Several studies have demonstrated[21,22] that when the percentage of ZrO_2 is kept under the 22 wt% in alumina composites, ageing phenomena does not occur independently from the grain size. Since the most promising materials in our work is the ATZ composite, especially after treatment in phosphoric acid, we studied the ageing process to calculate the real amount of phase transition and its effect on the mechanical properties with the aim to verify the effectiveness for in vivo applications. Fig. 5 shows the percentage in volume of the phase transition as a

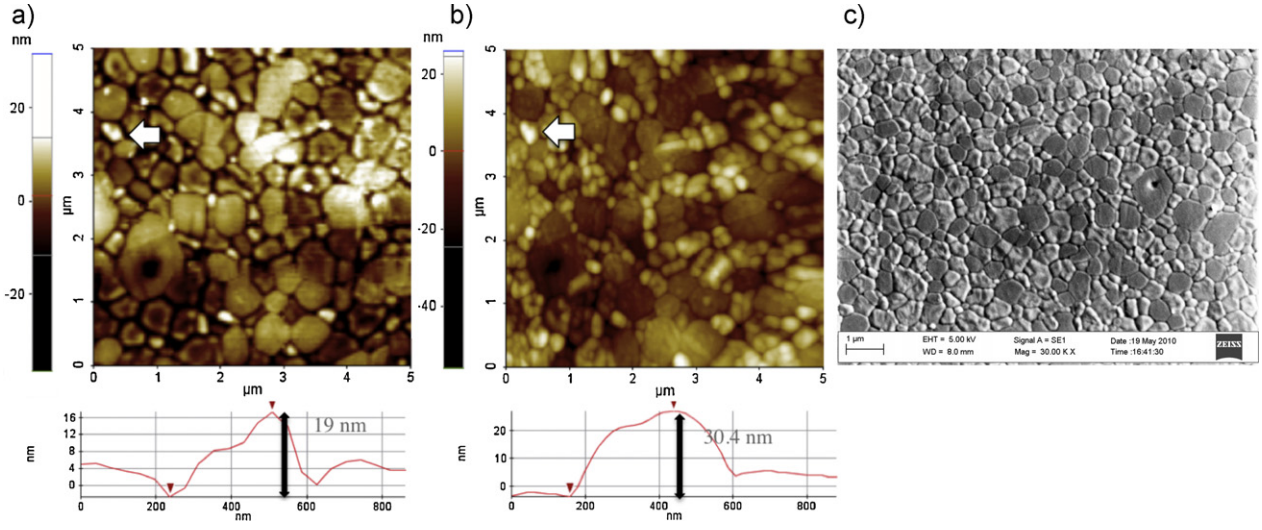

Fig. 6. AFM (left and middle) and SEM (right) images of the ATZ surface before the ageing process (a) and after 20 h of ageing in autoclave (b and c) for the same zone of the sample. Height profiles of the zirconia grain (indicating by an arrow) before and after the ageing process.

Table 4
Flexural strength values after different times of ageing of ATZ.

Material	Flexural strength 4 pt. (MPa)
ATZ as fired	1075 ± 190
ATZ aged in autoclave 20 h	1113 ± 142
ATZ aged in autoclave 90 h	1002 ± 40
ATZ treated by phosphoric acid and aged in autoclave for 20 h	1246 ± 124

function of the ageing time (up to 20 h, corresponding at 60–80 years in vivo, a time long enough for evaluating the duration of a prosthesis) for ATZ as fired and ATZ treated with phosphoric acid. The amount was calculated using the Garvie and Nicholson method, since it is widely used for similar works and, as a consequence, results obtained in literature[29,30] can be easily compared with ours. As for the as fired sample, it can be seen that the amount of monoclinic zirconia increases with the ageing time and the correlation is almost linear. The scattering of the data, obtained by repeating the measurements to limit errors, is contained. It can be seen that the phase transformation does not exceed the value of 28% in volume. Similar values were found also in other works[19] on aged samples, but the interest in our work was related to the observation that the treatment leading to bioactivity did not accelerate the ageing. More interestingly, ageing have not reduced the strength of ceramics after 20 h and phosphoric acid treatment leads in some way to an increase of the flexural strength (Table 4).

As for hardness, the effect of the treatment and ageing is shown in Fig. 7. Three different indentation loads have been used to check for any differences between bulk and surface. No significant differences were observed between surface and bulk in any case. Ageing has as main effect a progressive decreasing in hardness (Fig. 7b), whereas no clear trend is observed in the case of materials aged after treatment in phosphoric acid up to 20 h. A significant decrease is clearly visible after 90 h (Fig. 7c).

Comparison of the surfaces before and after 20 h of ageing are reported in Fig. 6a and b (AFM) and c (SEM), in which the same area can be observed. SEM image helps principally to distinguish the zirconia (bright) and alumina (dark) grains, even if it is possible to see a relief difference on the zirconia grains, since the SEM does not allow to determine a height increase. However it is possible to observe that the relief of a zirconia grain is modified; there are a grows of micrograins on the main surface grains with respect to unaged materials. The AFM images obtained before and after the ageing process clearly show a big difference in contrast. This modification on the AFM contrast is directly due to a height increase of zirconia grains after the ageing process.[38] On the zirconia grains presenting a phase transformation tetragonal to monoclinic, one can observe a height increasing (shown by a brightening of the grain). The example of one zirconia grain (shown by an arrow) is highlighted in Fig. 6. The grain height increases from 19.9 nm to 30.5 nm after 20 h of ageing. However, one can note that the transformation induces a very low increase of the average roughness (5–6 nm).

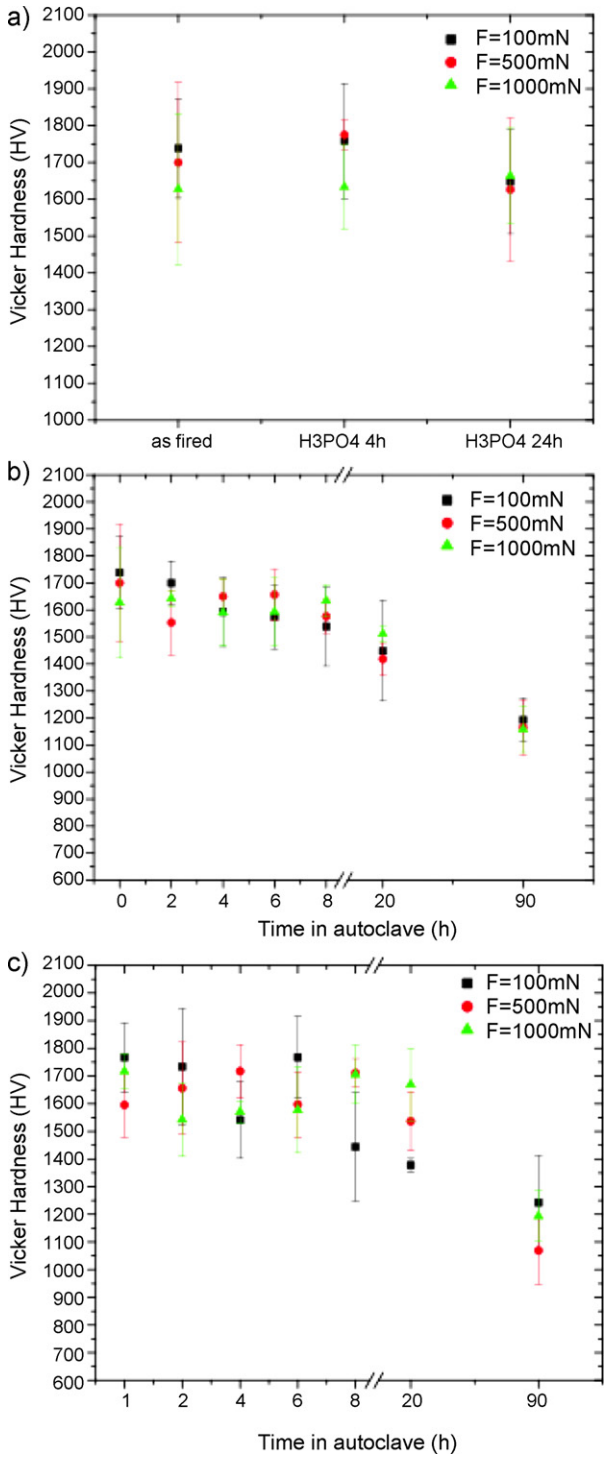

Fig. 7. Vickers micro-hardness (HV) at different applied loads of (a) as fired and acid-treated samples; (b) aged samples (ATZ as fired); (c) 4 h acid-treated samples after ageing.

4. Conclusion

Bioactivity of the composite with the highest percentage of zirconia (80 wt% zirconia, ATZ) was reached using a quick treatment (only 4 h) in phosphoric acid. Main mechanical properties and LTD resistance of the activated ATZ were also tested. Mechanical strength was slightly increased by the chemical

treatment that induced apatite formation. Also ageing did not resulted in a decrease of this important feature. This surface modified material can be then considered for applications in which both strength and bonding with bone are required, as dental implants and counter part of femoral heads.

References

1. Piconi C, Burger W, Richter HG, Cittadini A, Maccauro G, Covacci V, et al. Y-TZP ceramics for artificial joint replacements. *Biomaterials* 1998;**19**:1489–94.
2. Clarke I, Manaka M, Green D, Williams P, Pezzotti G, Kim Y, et al. Current status of zirconia used in total hip implants. *J Bone Joint Surg Am* 2003;**85-A**:73–84.
3. Chevalier J, Gremillard L. Ceramics for medical applications: a picture for the next 20 years. *J Eur Ceram Soc* 2009;**29**:1245–55.
4. Chevalier J. What future for zirconia as a biomaterial. *Biomaterials* 2006;**27**:535–43.
5. Kelly JR, Denry I. Stabilized zirconia as a structural ceramic: an overview. *Dent Mater* 2008;**24**:289–98.
6. Denry I, Kelly JR. State of the art of zirconia for dental applications. *Dent Mater* 2008;**24**:299–307.
7. Deville S, Guénin G, Chevalier J. Martensitic transformation in zirconia: part II. Martensite growth. *Acta Mater* 2004;**52**:5709–21.
8. Deville S, Chevalier J. Martensitic relief observation by atomic force microscopy in yttria-stabilized zirconia. *J Am Ceram Soc* 2003;**86**: 2225–7.
9. Chevalier J, Cales B, Drouin JM. Low-temperature aging of Y-TZP ceramics. *J Am Ceram Soc* 1999;**82**:2150–4.
10. Chevalier J, Gremillard L, Deville S. Low-temperature degradation of zirconia and implications for biomedical implants. *Annu Rev Mater Res* 2007;**37**:1–32.
11. Lawson S. Environmental degradation of zirconia ceramics. *J Eur Ceram Soc* 1995;**15**:485–502.
12. Guo X. On the degradation of zirconia ceramics during low-temperature annealing in water or water vapor. *J Phys Chem Solids* 1999;**60**: 539–46.
13. Basu D, Dasgupta A, Sinha MK, Sarkar BK. Low-temperature aging of zirconia toughened alumina under humid conditions. *Ceram Int* 1995;**21**:277–82.
14. Schubert H, Frey F. Stability of Y-TZP during hydrothermal treatment: neutron experiments and stability considerations. *J Eur Ceram Soc* 2005;**25**:1597–602.
15. Affatato S, Testoni M, Cacciari GL, Toni A. Mixed-oxides prosthetic ceramic ball heads. Part II: effect of the ZrO_2 fraction on the wear of ceramic on ceramic joints. *Biomaterials* 1999;**20**:1925–9.
16. De Aza AH, Chevalier J, Fantozzi G, Schehl M, Torrecillas R. Crack growth resistance of alumina, zirconia and zirconia toughened alumina ceramics for joint prostheses. *Biomaterials* 2002;**23**:937–45.
17. Kim DJ, Lee MH, Lee DY, Han JS. Mechanical properties, phase stability, and biocompatibility of (Y,Nb)-TZP/Al_2O_3 composite abutments for dental implant. *J Biomed Mater Res* 2000;**53**:438–43.
18. Moraes MCCS, Elias CN, Duailibi Filho J, Oliveira LG. Mechanical properties of alumina–zirconia composites for ceramic abutments. *Mater Res* 2004;**7**:643–9.
19. Nevarez-Rascon A, Aguilar-Elguezabal A, Orrantia E, Bocanegra-Bernal MH. On the wide range of mechanical properties of ZTA and ATZ based dental ceramic composites by varying the Al_2O_3 and ZrO_2 content. *Int J Refract Met Hard Mater* 2009;**27**:962–70.
20. Nevarez-Rascon A, Aguilar-Elguezabal A, Orrantia E, Bocanegra-Bernal MH. Al_2O_3(w)–Al_2O_3(n)–ZrO_2 (TZ-3Y)n multi-scale nanocomposite: an alternative for different dental applications. *Acta Biomater* 2010;**6**:563–70.
21. Deville S, Chevalier J, Fantozzi G, Bartolomé JF, Requena J, Moya JS, et al. Low-temperature ageing of zirconia-toughened alumina ceramics and its implication in biomedical implants. *J Eur Ceram Soc* 2003;**23**:2975–82.
22. Pecharromán C, Bartolomé J, Requena J, Moya J, Deville S, Chevalier J, et al. Percolative mechanism of aging in zirconia-containing ceramics for medical applications. *Adv Mater* 2003;**15**:507–11.
23. Chevalier J, Grandjean S, Kuntz M, Pezzotti G. On the kinetics and impact of tetragonal to monoclinic transformation in an alumina/zirconia composite for arthroplasty applications. *Biomaterials* 2009;**30**:5279–82.
24. Kokubo T, Takadama H. How useful is SBF in predicting in vivo bone bioactivity. *Biomaterials* 2006;**27**:2907–15.
25. Kokubo T, Matsushita T, Takadama H, Kizuki T. Development of bioactive materials based on surface chemistry. *J Eur Ceram Soc* 2009;**29**:1267–74.
26. Uchida M, Kim HM, Kokubo T, Nawa M, Asano T, Tanaka K, et al. Apatite-forming ability of a zirconia/alumina nano-composite induced by chemical treatment. *J Biomed Mater Res* 2002;**60**:277–82.
27. Li P, Ohtsuki C, Kokubo T, Nakanishi K, Soga N, de Groot K. The role of hydrated silica, titania, and alumina in inducing apatite on implants. *J Biomed Mater Res* 1994;**28**:7–15.
28. Uchida M, Kim H-M, Kokubo T, Miyaji F, Nakamura T. Bonelike apatite formation induced on zirconia gel in a simulated body fluid and its modified solutions. *J Am Ceram Soc* 2001;**84**:2041–4.
29. Garvie RC. Phase analysis in zirconia systems. *J Am Ceram Soc* 1972;**55**:303.
30. Toraya H, Yoshimura M, Somiya S. Calibration curve for quantitative analysis of the monoclinic-tetragonal ZrO_2 system by X-ray-diffraction. *J Am Ceram Soc* 1984;**67**:C119–21.
31. Damyanova S, Grange P, Delmon B. Surface characterization of zirconia-coated alumina and silica carriers. *J Catal* 1997;**168**:421–30.
32. Morant C, Sanz JM, Galán L, Soriano L, Rueda F. An XPS study of the interaction of oxygen with zirconium. *Surf Sci* 1989;**218**:331–45.
33. Parmigiani F, Depero LE, Sangaletti L, Samoggia G. An XPS study of yttria-stabilised zirconia single crystals. *J Electron Spectrosc Relat Phenom* 1993;**63**:1–10.
34. Alexander MR, Thompson GE, Beamson G. Characterization of the oxide/hydroxide surface of aluminium using X-ray photoelectron spectroscopy: a procedure for curve fitting the O 1s core level. *Surf Interface Anal* 2000;**29**:468–77.
35. Crist BV. *Handbooks of monochromatic XPS spectra, the element of native oxide*. New York: Wiley; 2000.
36. Delebecque A, Thomas C, Methivier C, Coffre E, Paoli H, Carre M. Reactivity of a hydroxylated alumina surface in the presence of NO diluted in N_2: a PM-IRRAS in situ investigation. *J Phys Chem C* 2008;**112**:2964–71.
37. Klopcic SB, Kovac J, Kosmac T. Apatite-forming ability of alumina and zirconia ceramics in a supersaturated Ca/P solution. *Biomol Eng* 2007;**24**:467–71.
38. Deville S, Chevalier J, Dauvergne C, Fantozzi G, Bartolomé JF, Moya JS, et al. Microstructural investigation of the aging behavior of (3Y-TZP)-Al_2O_3 composites. *J Am Ceram Soc* 2005;**88**:1273–80.